SEPTEMBER 01 2006

Diffraction of sound due to moving sources by barriers and ground discontinuities

M. Buret; K. M. Li; K. Attenborough

J. Acoust. Soc. Am. 120, 1274–1283 (2006)
https://doi.org/10.1121/1.2221535

Diffraction of sound due to moving sources by barriers and ground discontinuities

M. Buret and K. M. Li[a)]
Department of Mechanical Engineering, The Hong Kong Polytechnic University, Hung Hom, Hong Kong

K. Attenborough
Department of Engineering, The University of Hull, Cottingham Road, Hull HU6 7RX, United Kingdom

(Received 2 December 2005; revised 14 June 2006; accepted 14 June 2006)

The solution for diffraction of sound by a wedge is extended to sources in uniform motion parallel to the obstacle. By means of an auxiliary transformation the problem is reduced to that of a set of stationary sources so that the resulting solution is in accordance with well-known models. Applications to prediction and abatement of transportation noise are considered. The formulation for the diffracted wave is combined with the solution for ground reflection of sound due to moving sources. New models for the sound field due to a source in motion along a barrier above the ground and for a source moving parallel to an impedance discontinuity are derived. In both situations, greater sensitivity to motion of the resulting sound pressure levels is found on source approach. However, attenuation of sound from moving sources by barriers is found to be so little affected by motion that design schemes for stationary source are relevant. On the other hand, it is noted that noise predictions must account for source motion. © *2006 Acoustical Society of America.*
[DOI: 10.1121/1.2221535]

PACS number(s): 43.28.Js, 43.28.Fp, 43.20.Dk, 43.20.El [VEO] Pages: 1274–1283

I. INTRODUCTION

Diffraction by obstacles is a common problem in wave physics and fundamental solutions in acoustics have been derived by borrowing from other fields such as electromagnetics.[1] Since they are a traditional means for noise abatement, an obvious acoustical application is to noise barriers.

Although simplified schemes[2,3] are generally considered sufficient for predicting noise barrier efficiency, their scope is usually limited to basic situations such as stationary omnidirectional point sources in the presence of nonabsorptive surfaces. In more complex cases, although semiempirical approaches can lead to analytical models,[4] it is necessary to consider the theoretical foundation of the problem, particularly when higher accuracy is sought.

Pierce[5] has treated the classic problem of sound wave diffraction by wedges. In particular he relates the solution to the general context of the geometrical theory of diffraction. This solution has been extended to situations relevant to environmental noise predictions and abatement such as wide barriers,[5] barriers above impedance ground and impedance discontinuities,[6] and the diffraction of sound by absorbing barriers.[7] However, except for a recent formulation for diffraction of sound due to dipoles[8] and a unifying model for point sources, point source arrays and line sources,[9] few works have focused on extension of the models at the source end.

In particular, to the authors' knowledge, little can be found on the diffraction of sound due to moving sources. Noise prediction schemes typically neglect the Doppler and convection effects related to source motion.[10] For barriers in urban areas, involving high traffic density and speed restrictions, it possible to neglect the Doppler and convection effects when formulating the expressions for the sound field. However, for high speed trains, which can reach speeds beyond 400 km/h, these assumptions are less acceptable.

In this context, an expression—hereinafter referred to as the *Doppler-Weyl-Van der Pol formula*—was recently introduced by Buret *et al.*[11,12] for the sound field due to a source at high speed motion above the ground. Following Morse and Ingard's method[13,14] for deriving the sound field due to a source in uniform motion, use of an auxiliary coordinate system in well-known expressions for stationary sources, enabled the problem to be tackled from the governing equations. It was shown that, although moderate, the effects of source motion were significant even for relatively low Mach numbers.

In this paper, a similar approach is used to derive the expression for the sound wave due to a source in motion in the presence of a barrier—or a diffracting element, extending Pierce's expression.[5] The derivation of this fundamental solution is presented in Sec. II. Section III is dedicated to applications of the new model to situations relevant to environmental acoustics. First, the effects of motion on barrier attenuation are discussed; the sound field due to a moving source in the presence of a hard screen above arbitrary ground is then derived. Eventually, De Jong *et al.*'s model for propagation of sound in the presence of a ground discontinuity[6] is extended to account for source motion.

[a)]Corresponding author. Present address: Ray W. Herrick Laboratories, School of Mechanical Engineering, Purdue University, 140 S. Intramural Drive, West Lafayette, IN 47907-2031. Electronic mail: mmkmli@purdue.edu

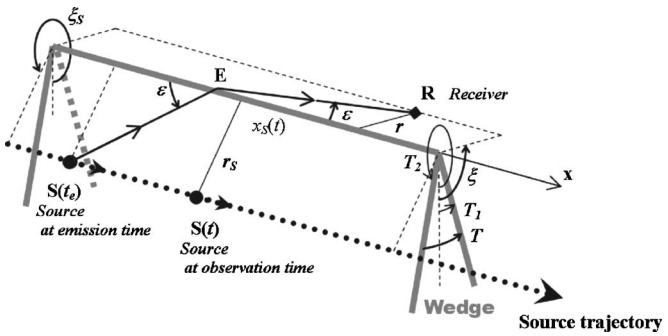

FIG. 1. Geometry for a source S in uniform motion along a semi-infinite wedge of top angle T. The x axis coincides with the edge of the wedge and the cylindrical coordinates of the source $[\xi_S, r_S, x_S(t)]$ and the motionless receiver R located at (ξ, r, x) are explicated. The diffracted ray is represented by the broken segment $S(t_e)$-E-R.

II. DIFFRACTION OF SOUND DUE TO A POINT SOURCE IN UNIFORM MOTION ALONG A RIGID WEDGE

A. Kinematics

Consider a semi-infinite rigid wedge with constant cross section in the vertical plane y-z. Its faces are oriented at arbitrary angles T_1 and T_2 ($T_1 < T_2$) with respect to the latter (see Fig. 1). The top angle of the wedge is $T = 2\pi + T_1 - T_2$ and takes the value $2T_1$ in the particular case of a symmetrical wedge. Let S be a sound source moving along the x axis, hence, in parallel to the edge of the wedge. A cylindrical coordinate system (ξ, r, x) attached to a motionless receiver can be introduced, in which $\mathbf{r_s} \equiv (\xi_S, r_S, x_S)$ represents the source coordinates. For uniform source motion at Mach number M, the only varying parameter is the source-receiver offset x-x_S. Let the initial position of the source be located at $x=0$ and c_0 be the speed of sound; then

$$x_S(t) = c_0 M t. \tag{1}$$

The projection of the geometry in the cross-sectional plane y-z remains unchanged with source motion and the analogy with a stationary source and/or a two-dimensional situation is then obvious. According to the geometrical theory of diffraction, the diffracted sound ray is a segment linking the source S to the receiver R via the edge of the wedge E. The diffracted path length is then $L = \overline{SE} + \overline{ER}$ The diffraction angle ε is the same on both source and receiver side.[5] Let the receiver be motionless and located at cylindrical coordinates $(\xi, r, 0)$; then

$$\cos\varepsilon = -\frac{c_0 M t_e}{L}, \quad \sin\varepsilon = \frac{r + r_s}{L}, \quad x_E = -\frac{r}{\tan\varepsilon}, \tag{2}$$

where t_e is the time of emission of the diffracted wave reaching the receiver at time t, L is the total length of the diffracted ray, and x_E defines the position E at which the diffracted ray intersects the edge of the wedge. L and t_e are the solutions of

$$c_0(t - t_e) = L = \sqrt{(r + r_S)^2 + (c_0 M t_e)^2}, \tag{3}$$

which resolves as

$$t_e = \frac{c_0 - \Lambda}{c_0(1 - M^2)}, \quad L = \frac{\Lambda - M(c_0 M t)}{1 - M^2}, \tag{4a}$$

$$\Lambda = \sqrt{(c_0 M t)^2 + (1 - M^2)(r + r_S)^2} = L(1 - M_E), \tag{4b}$$

where $M_E = M\cos\varepsilon$ is the component of the Mach number along the diffracted ray.

B. Diffracted pressure for a source in uniform motion

In the case of a stationary point source, the pressure field in the vicinity of a wedge can be expressed as the sum of up to four components:[5] a direct pressure field p_{dir}, two reflections on the faces of the wedge $p_{\text{refl},1}$ and $p_{\text{refl},2}$, and a diffracted wave p_{diffr}. The three first contributions may or may not occur, depending on the relative source and receiver positions with respect to the wedge that may screen the sound source or its images from the receiver[5,8]

$$p = U[\pi - |\xi - \xi_S|]p_{\text{dir}} + U[\pi + 2T_1 - (\xi + \xi_S)]p_{\text{refl},1} + U[(\xi + \xi_S) + \pi - 2T_2]p_{\text{refl},2} + p_{\text{diffr}}. \tag{5}$$

In Eq. (5), the Heaviside step function U ($U[x]=1$ if $x>0$; $U[x]=0$ if $x\leqslant 0$) determines the presence or absence of the direct and reflected waves. Remarkably, the arguments of U—and thence the composition of the sound field—depend only on the angular coordinates of the source, the receiver, and the faces of the wedge in the cross-sectional plane.

In the case of a source moving parallel to the edge of a wedge, the geometry in this plane remains constant and therefore the relationships determining the presence or absence of the direct and reflected pressure waves remain the same as in Eq. (5). When present, the direct wave is expressed as the pressure due to the source in motion in the free field.[13,14] The potential contributions due to the reflected waves can be formulated considering either a formulation for reflection of the sound field due to a source in motion above a plane,[11] or the acoustic pressure field due to the relevant image sources with respect to the faces of the wedge radiating in the absence of obstacle. Derivation of these contributions is straightforward and will not be detailed here for brevity, and because in practical applications (noise barriers), the sound field is composed of the diffracted wave only.

Morse and Ingard have derived the sound field due to a monopole in uniform motion in the free field by means of an auxiliary transformation, analogous to a Lorentz transformation.[13] Buret *et al.*[11] have used the same transformation to formulate the Doppler-Weyl-Van der Pol formula for a source moving above an impedance ground. The coordinates and time (x_L, y_L, z_L, t_L) in the auxiliary coordinate system are

$$\begin{aligned} x_L &= \gamma^2(x - c_0 M t), \\ y_L &= \gamma y, \\ z_L &= \gamma z, \\ t_L &= \gamma^2(t - Mx/c_0), \end{aligned} \quad \text{with } \gamma = 1/\sqrt{1 - M^2}. \tag{6}$$

Hereinafter, subscript L characterizes corresponding variables in the auxiliary coordinate system. In the case of uniform source motion, the wave equation for the velocity po-

tential field φ takes the same form as that for a stationary monopole when expressed in the auxiliary coordinate system.[13] The acoustic pressure is then calculated as the time derivative of the velocity potential[13] $p=\rho\partial\varphi/\partial t$ where ρ is the air density. Noting that

$$\frac{\partial}{\partial t}=\gamma^2\frac{\partial}{\partial t_L}-\gamma^2 c_0 M\frac{\partial}{\partial x_L}, \tag{7}$$

it is shown that the acoustic pressure field can be expressed as the sum of contributions from two stationary sources: a monopole and a dipole oriented in the direction of source motion.[12] Denoting these relative contributions by $p^{(0)}$ and $p^{(1)}$, respectively, the total pressure p due to a harmonic source of strength P_0 can be expressed as[11]

$$p=P_0\left(\gamma^4 p^{(0)}-\gamma^4\frac{M}{ik_0}p^{(1)}\right), \tag{8}$$

where k_0 is the wave number, $k_0=\omega/c_0$, ω being the angular frequency of the source.

With constant Mach number, the auxiliary transformation involves uniform expansion along the three dimensions, as well as a time dependent translation along the direction x of source motion. As a result, the transformed geometry is analogous to that for a stationary source in the original coordinate system. A cylindrical coordinate system (ξ_L,r_L,x_L) is introduced, relating to that attached to the motionless receiver by

$$\xi_L=\xi,\quad r_L=\gamma r,\quad x_L=\gamma^2(x-c_0Mt). \tag{9}$$

Remarkably, the polar angle is unaffected by the transformation. As a result, the top angle of the wedge has same value in both the auxiliary and original coordinate system. Using Pierce's formulation,[5,15] the expression for the monopole component of the diffracted wave is

$$p^{(0)}=\frac{\exp[-i\omega(t_L-L_L/c_0)]}{4\pi L_L}\frac{e^{i\pi/4}}{\sqrt{2}}[A_D(X_{L+})+A_D(X_{L-})], \tag{10a}$$

where L_L is the diffracted path in the transformed coordinates and A_D is the diffraction integral

$$A_D(X_{L\pm})=\frac{1}{\pi\sqrt{2}}\int_{-\infty}^{\infty}\frac{e^{-u^2}}{(\pi/2)^{1/2}X_{L\pm}-e^{-i\pi/4}u}du, \tag{10b}$$

$$X_{L\pm}=\Gamma_L N_\nu(\alpha_\pm),\quad \alpha_-=\xi+\xi_S-2T_1,\quad \alpha_+=\xi-\xi_S, \tag{10c}$$

$$\Gamma_L=\sqrt{k_0 r_L\rho_S/\pi L_L},\quad N_\nu(\alpha_\pm)=\frac{\cos\nu\pi-\cos\nu\alpha_\pm}{\nu\sin\nu\pi}, \tag{10d}$$

where $\nu=\pi/(2\pi-T)$ is the wedge index and $\rho_S=\gamma r_S$.

The expression for the three-dimensional (3D) dipole field diffracted by a wedge has been derived and has been validated by laboratory measurements elsewhere.[8] For a dipole lying along the x_L axis, the sound field can be expressed using[8,16]

$$p^{(1)}=\frac{\exp[-i\omega(t_L-L_L/c_0)]}{4\pi L_L}\frac{\cos\varepsilon_L}{L_L}\frac{e^{i\pi/4}}{\sqrt{2}}\Bigg\{(1-ik_0L_L)\times[A_D(X_{L+})+A_D(X_{L-})]+\frac{i}{2}[X_{L+}(1-\pi X_{L+}A_D(X_{L+}))+X_{L-}(1-\pi X_{L-}A_D(X_{L-}))]\Bigg\}. \tag{11}$$

Both X_{L^+} and X_{L^-}take small values for long diffraction paths and high frequencies. As a result, the second term inside the curly brackets in Eq. (11) can be neglected.[8] This approximation is particularly applicable for source motion in parallel to the edge of the wedge, as the diffracted path length increases with the time-dependent source-receiver offset x-x_S. The dipole component of the pressure then takes a form similar to the monopole pressure given in Eq. (10), except for the directivity coefficient $\cos\varepsilon_L$ and the strength factor $(1-ik_0L)/L_L$,

$$p^{(1)}=\frac{\exp[-i\omega(t_L-L_L/c_0)]}{4\pi L_L}\frac{\cos\varepsilon_L}{L_L}\frac{e^{i\pi/4}}{\sqrt{2}}(1-ik_0L_L)\times[A_D(X_{L+})+A_D(X_{L-})]. \tag{12}$$

The total diffracted pressure is then expressed by substituting Eqs. (10) and (12) into Eq. (8),

$$p=\gamma^4P_0\frac{\exp[-i\omega t_L]}{4\pi}\frac{\exp(ik_0L_L)}{L_L}\frac{e^{i\pi/4}}{\sqrt{2}}\times\left[1+M\cos\varepsilon_L\left(1-\frac{1}{ik_0L_L}\right)\right][A_D(X_{L+})+A_D(X_{L-})]. \tag{13}$$

Transforming back into the coordinate and time system (x,y,z,t) attached to the receiver is straightforward, noting that

$$L_L=\sqrt{(\gamma r+\gamma r_S)^2+x_L^2}=\gamma^2L(1-M\cos\varepsilon), \tag{14a}$$

$$t_L-\frac{L_L}{c_0}=t_e=t-\frac{L}{c_0}, \tag{14b}$$

and

$$\cos\varepsilon_L=\frac{x_L}{L_L}=\frac{\cos\varepsilon-M}{1-M\cos\varepsilon}. \tag{14c}$$

The diffracted acoustic pressure wave due to a monopole in uniform motion in parallel to a rigid wedge is represented by

$$p=P_0\frac{\exp(-i\omega t)}{4\pi}\frac{\exp(ik_0L)}{L(1-M\cos\varepsilon)^2}\times\left\{\frac{e^{i\pi/4}}{\sqrt{2}}\left[1-\frac{1}{ik_0L}\frac{M\cos\varepsilon-M^2}{1-M\cos\varepsilon}\right]\left[A_D\left(\frac{X_+}{\sqrt{1-M\cos\varepsilon}}\right)+A_D\left(\frac{X_-}{\sqrt{1-M\cos\varepsilon}}\right)\right]\right\}, \tag{15}$$

where A_D is defined as in Eq. (10b) with

$$X_\pm=\Gamma N_\nu(\alpha_\pm),\quad \Gamma=\sqrt{k_0 r r_S/\pi L}. \tag{16}$$

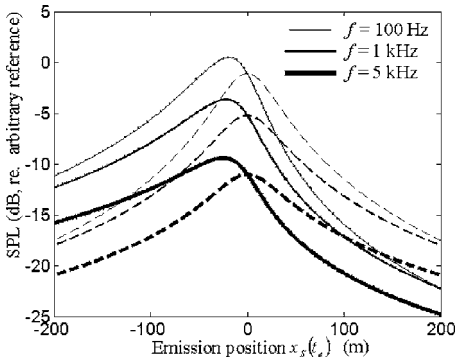

FIG. 2. Diffracted pressure for a source in uniform motion at Mach 0.3 along a half plane at discrete frequencies 100 Hz (thin lines), 1 kHz (thick lines), and 5 kHz (thicker lines). Coinciding solid and dotted lines of the same thickness correspond to the approximate solution in Eq. (15) and the full expression with dipole component expressed using Eq. (11), respectively. Dashed lines correspond to predictions for the corresponding stationary source at position of emission. The source trajectory is 1 m below the edge, with horizontal separation 10 m; the receiver is 0.8 m below the edge at distance 20 m.

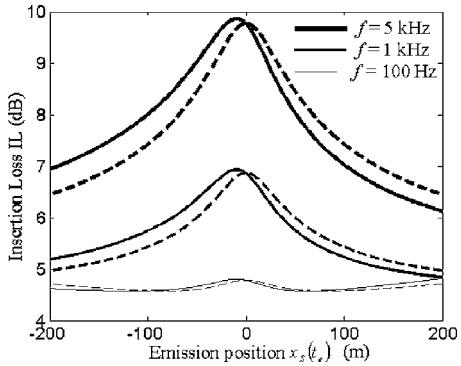

FIG. 3. IL for the same source and obstacle as for Fig. 2, for discrete frequencies 100 Hz (thin lines), 1 kHz (thick lines), and 5 kHz (thicker lines). Solid lines show the IL for a source moving at Mach number 0.3, dashed lines show the IL for the corresponding stationary source.

In Fig. 2, the sound pressure level (SPL) for the diffracted wave is plotted for discrete frequencies 100 Hz, 1 and 5 kHz, for a point source moving at Mach number 0.3 ($\sim$360 km/h which is a plausible speed for a high train, for example) in the vicinity of a semi-infinite rigid half plane ($T=0$; $\nu=1/2$) with source, receiver, and obstacle edge at heights 1, 1.2, and 2 m, respectively. The shortest horizontal separation from the obstacle to the source is 10 m and that to the receiver on the other side is 20 m. Coincident solid and dotted lines show, respectively, the results of calculations by means of the approximation in Eq. (15) and using the full dipole component given in Eq. (11). Such coincidence validates the approximation used to derive Eq. (15) along the whole source trajectory. Dashed lines show the SPL calculated for a *corresponding stationary source*—i.e., a stationary monopole located at the position $x_S(t_e)$ of emission. Comparison with the predictions for the moving source enables an assessment of the effects of source motion other than the geometrical change in location of the source position. The SPL is higher than for a stationary source when the source approaches the receiver $[x_S(t_e) \leqslant 0]$, and lower when it is receding $[x_S(t_e) \geqslant 0]$.

It should be noted that the maximum in SPL is predicted to occur when the source is approaching the receiver, hence, before the point of closest source-receiver approach. These effects are directly related to the Doppler factor $(1-M\cos\varepsilon)^{-1}$ and the convection coefficient $(1-M\cos\varepsilon)^{-2}$ in Eq. (15). Both are larger than 1 on approach—leading to higher pressure amplitude [cf. Eq. (15)]—and smaller than 1 on recession resulting in lower SPL. The shift of the peak towards the approaching source position is due to the nonlinearity (and, hence, nonsymmetry) of the logarithm function used to express the SPL in decibels (dB) while $(1-M\cos\varepsilon)$ shows symmetry around the value 1. These observations are consistent with previous results for a source moving in the absence of obstacles[13] for which similar observations can be made in accordance to variations in the Doppler factor around 1.

III. APPLICATIONS TO OUTDOOR ACOUSTICS

A. Effect of source motion on barrier attenuation

Barrier attenuation is typically characterized by the insertion loss (IL): the ratio in dB of the total pressure wave perceived at the receiver [Eq. (15)] to the direct sound field p_{dir} that would occur in the absence of any obstacle

$$\mathrm{IL} = -10\log[|p(t)/p_{\mathrm{dir}}(t)|]. \tag{17a}$$

In the case of a source in motion[11,13,14]

$$p_{\mathrm{dir}}(t) = P_0\frac{\exp(-i\omega t)}{4\pi}\frac{\exp(ik_0R)}{R(1-M\cos\psi\sin\phi)^2} \times\left[1-\frac{M}{ik_0R}\left(\frac{\cos\psi\sin\phi-M}{1-M\cos\psi\sin\phi}\right)\right], \tag{17b}$$

where R is the length of the direct source-receiver path, ψ and ϕ are its azimuthal and elevation angles, such that $\cos\psi\sin\phi=-x_S(t_{\mathrm{dir}})/R$, with $t_{\mathrm{dir}}=t-R/c_0$ the emission time of the direct wave. Due to the path difference between the direct and the diffracted wave the latter has been emitted earlier: $t_e<t_{\mathrm{dir}}$.

Figure 3 shows the IL predicted for the same source and receiver locations as in Fig. 2 and calculated for the same discrete frequencies. The solid lines show the IL predicted for a source moving at Mach number 0.3, whereas dotted lines show the IL predicted for the corresponding stationary source. The IL predicted for the moving source is within only 1 dB of that predicted for a stationary source. Recalling the expression for the diffracted wave given in Eq. (15), we point out that the magnitude of the IL depends strongly on the ratio of the convection factors $(1-M\cos\varepsilon)^2/(1-M\cos\psi\sin\phi)^2$. The latter is close to 1 when the path difference between direct and diffracted pressures is not large $(L/R\approx 1)$, which is the case for large source offset, for example. The expression for the magnitude of the IL due to a source in motion is then close to that for the corresponding stationary source, except for the Doppler factor in the argument of the diffraction integrals A_D. The general trend, showed clearly in Fig. 3 for 1 and 5 kHz is explained by the fact that the IL is predicted to increase with the argument of decreasing function A_D. When the source is approaching, the Doppler factor $(1-M\cos\varepsilon)^{-1}$ is greater than 1 and the pre-

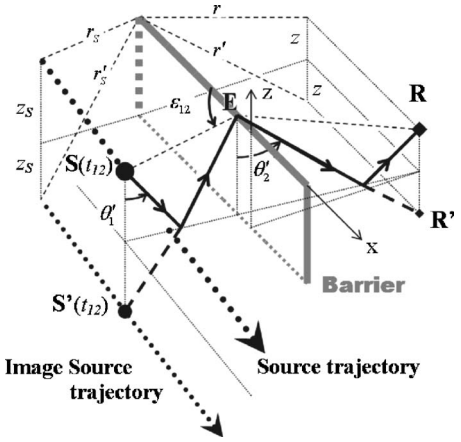

FIG. 4. Geometry for a source in uniform motion in parallel to a thin barrier above the ground. The diffraction path "12" with reflection on both sides of the barrier is represented by thick lines.

dicted insertion loss for a source in motion will be larger than for a stationary source located at the point of emission $x_S(t_e)$. This trend is reversed when the source recedes from the receiver, with smaller predicted IL than in the motionless case.

The predicted influences of the Doppler and convection factors on the barrier attenuation are small and the effects of motion on the IL are mainly related to the change in source position over the trajectory. It can be concluded therefore that usual schemes to estimate barrier attenuation for stationary sources—such as Maekawa's[3]—can apply to screen design in situations involving sources in motion, particularly at low speed.

On the other hand, for the sake of accuracy, noise predictions must account for source displacement and convection in order to properly describe the absolute pressure field. As shown in Fig. 2, the maximum in predicted SPL occurs before the source reaches the shortest separation to the receiver, hence, the resulting sound field is somewhat affected by source motion and it is necessary to account for the convection and Doppler effects in its formulation. For typical outdoor situations it is important to allow for the presence of ground around the barrier. This is the subject of the next section. A further related analysis of the effects of ground discontinuity on the sound field of a moving source follows this.

B. Barrier in the presence of ground

Sound propagation around a rigid barrier on the ground is a classical problem. In the case of hard ground on both sides of the barrier, the solution may be obtained in a straightforward manner by means of mirror images. When the source is screened from the receiver, the total sound field is the sum of the four diffracted waves, corresponding to the paths linking the source S and its image S' with respect to the ground to the receiver R and its image R' via the top edge of the barrier (Fig. 4). Denoting with subscript 1 the paths including a reflection on the source side and by subscript 2 those for which there is a reflection on the receiver side

$$p = p_0 + p_1 + p_2 + p_{12}, \tag{18}$$

where p_0 stands for the diffracted wave obtained for path 0, linking source to edge to receiver with no ground reflection. Subscript $K \equiv 0,1,2,12$ is used in the following for general formulas valid for all four diffraction paths.

Using the same reference systems as in Sec. II, the coordinate vectors of the image source and the image receiver are $\mathbf{r}'_S$ and $\mathbf{r}'$, respectively. In the Cartesian coordinate system (x,y,z):

$$\mathbf{r}'_S(t) \equiv (-c_0 M t,\, y_S, -z_S), \quad \mathbf{r}'(t) \equiv (0, y, -z), \tag{19a}$$

whereas in the cylindrical coordinate system (r,ξ,x):

$$\mathbf{r}'_S(t) \equiv (r'_S, 2\pi - \xi_S, -c_0 M t), \quad \mathbf{r}'(t) \equiv (r', 2\pi - \xi, 0). \tag{19b}$$

Let z_E be the barrier height; then

$$r'_S = r_S \sqrt{1 - 4\frac{z_E}{r_S}\left(\cos\xi_S - \frac{z_E}{r_S}\right)}, \tag{20a}$$

$$r' = r \sqrt{1 - 4\frac{z_E}{r}\left(\cos\xi - \frac{z_E}{r}\right)}. \tag{20b}$$

Obviously the four diffracted paths have different lengths and as a result, each contribution in Eq. (18) has been emitted at a different time t_K, solution of

$$L_K = c_0(t - t_K), \tag{21a}$$

where the L_K's are the diffracted path lengths

$$L_0 = \sqrt{(r_S + r)^2 + (c_0 M t_0)^2},$$

$$L_1 = \sqrt{(r'_S + r)^2 + (c_0 M t_1)^2},$$

$$L_2 = \sqrt{(r_S + r')^2 + (c_0 M t_2)^2},$$

$$L_{12} = \sqrt{(r'_S + r')^2 + (c_0 M t_{12})^2}. \tag{21b}$$

The components of the Mach number in the direction of the diffracted rays M_K's are determined from the diffraction angles ε_K by

$$M_K = M\cos\varepsilon_K = -M\frac{c_0 M t_K}{L_K}. \tag{22}$$

Solving Eq. (21), each pressure wave component is calculated from Eq. (15), substituting the appropriate (image) source and (image) receiver coordinates, as well as the corresponding diffracted path and angle, L_K and ε_K. The total pressure is then calculated by substitution into Eq. (18).

In the presence of soft ground on either or both source and receiver side of the barrier, the corresponding reflection coefficients differ from 1 (hard ground). Equation (18) must be amended to account for ground reflections.[4] It is then necessary to consider the monopole and dipole components of the pressure field as expressed in Eq. (8) separately. Let β_1 and β_2 be the admittance of the ground on the source and receiver side, respectively. As in the previous section, subscript 1 denotes a reflection on the source side, whereas subscript 2 corresponds to a reflection on the receiver side.

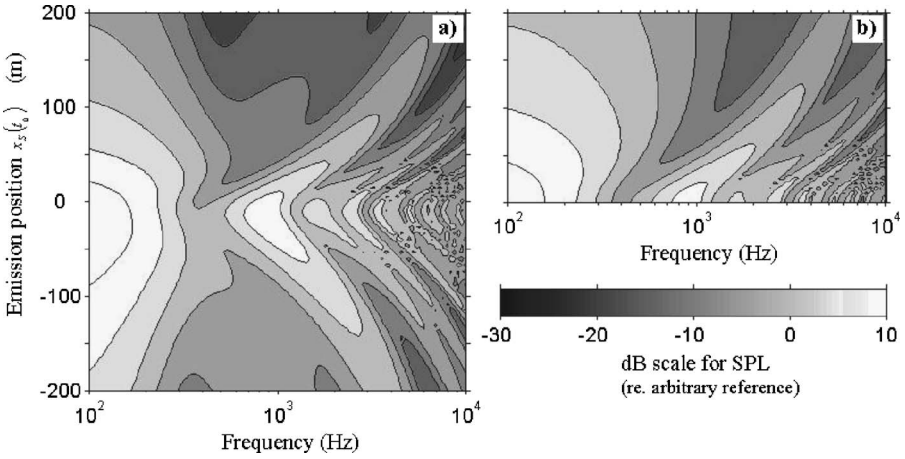

FIG. 5. (a) Sound field due to a source moving at Mach number 0.3 along a thin barrier of height 2 m. The source path is 10 m away from the barrier, at height 1 m. The receiver is in the shadow zone, 20 m away from the barrier and at height 1.2 m. The ground is hard ground on the source side and soft ground (σ_e =140 kPa s m^{-2} and α_e=35 m^{-1}) on the receiver side. (b) Sound field due to a corresponding stationary source in the same geometry as (a), with offset varying from 0 to 200 m.

The monopole component expressing the sound field due to a stationary monopole in the presence of a barrier over the ground is given by Jonasson.[4] In the auxiliary coordinates

$$p^{(0)} = p_0^{(0)} + Q_1 p_1^{(0)} + Q_2 p_2^{(0)} + Q_1' Q_2' p_{12}^{(0)}. \tag{23}$$

The diffracted monopole pressures $p_K^{(0)}$ are calculated after Eq. (10). Dashes on the reflection coefficients applied to the last term of Eq. (23) denote the fact that the emission time for p_{12} is different from those for p_1 and p_2. In accordance with Huygens's principle that considers the diffracted wave as emitted by a secondary source located at the edge of the obstacle,[5] the spherical wave reflection coefficients are calculated for the paths joining the image source and the image receiver to the edge of the barrier,[7] respectively

$$\rho_1 = \frac{r_S'}{r + r_S'} L_1,$$

$$\rho_2 = \frac{r'}{r' + r_S} L_2, \quad \rho_1' = \frac{r_S'}{r' + r_S'} L_{12}, \quad \rho_2' = \frac{r'}{r' + r_S'} L_{12}. \tag{24}$$

Use of the Doppler-Weyl Van der Pol formula,[11] with $i \equiv 1,2$, gives

$$Q_i = R_{Pi} + (1 - R_{Pi}) F\left(\frac{w_i}{\sqrt{1 - M_i}}\right), \quad M_i = M \cos \varepsilon_i, \tag{25a}$$

where R_{Pi} is the plane wave reflection coefficient

$$R_{Pi} = \frac{\cos \theta_i - \beta_i}{\cos \theta_i + \beta_i}, \tag{25b}$$

and F is the boundary loss function

$$F\left(\frac{w_i}{\sqrt{1 - M_i}}\right) = 1 + i\sqrt{\pi} \frac{w_i}{\sqrt{1 - M_i}} \exp\left(-\frac{w_i^2}{1 - M_i}\right) \times \operatorname{erfc}\left(-i \frac{w_i}{\sqrt{1 - M_i}}\right), \tag{25c}$$

where erfc is the complementary error function and w_i is the numerical distance,

$$w_i = \left(-\tfrac{1}{2} i k_0 \rho_i\right)^{1/2} (\cos \theta_i + \beta_i), \tag{25d}$$

$$\cos \theta_1 = (z_S + z_E)/\rho_1, \quad \cos \theta_2 = (z + z_E)/\rho_2. \tag{25e}$$

Equations (25a)–(25e) hold for the calculation of Q_1' and Q_2' after substituting dashed parameters.

The dipole component of the pressure field is expressed in the auxiliary coordinate system, recalling the solution for the stationary dipole by Buret *et al.*[8] For a dipole along the x_L axis

$$p^{(1)} = p_0^{(1)} + Q_1 p_1^{(1)} + Q_2 p_2^{(1)} + Q_1' Q_2' p_{12}^{(1)} + \frac{\partial Q_1}{\partial x_S} p_1^{(0)} + \frac{\partial Q_1'}{\partial x_S} Q_2' p_{12}^{(0)}, \tag{26}$$

where the same notations as in Eq. (23) are used, with superscript (1) denoting pressure due to dipole sources. The diffracted pressures $p_K^{(1)}$ are calculated after Eq. (12). The last two terms in Eq. (26) involving the diffracted monopole pressures $p_1^{(0)}$ and $p_{12}^{(0)}$ can be neglected due to small variations of the spherical wave reflection coefficient in the horizontal plane. The acoustic pressure field due to a point source moving along a barrier over arbitrary ground is then straightforward, summing the monopole and the dipole contributions and transforming back into the coordinate system attached to the receiver

$$p = p_0 + Q_1 p_1 + Q_2 p_2 + Q_1' Q_2' p_{12}, \tag{27}$$

$$p_K = P_0 \frac{\exp(-i\omega t)}{4\pi} \frac{\exp(i k_0 L_K)}{L_K (1 - M \cos \varepsilon_K)^2} \times \left\{ \frac{1 + i}{2} \left[1 - \frac{1}{i k_0 L_K} \frac{M \cos \varepsilon_K - M^2}{1 - M \cos \varepsilon_K} \right] \left[A_D\left(\frac{X_{K+}}{\sqrt{1 - M \cos \varepsilon_K}}\right) + A_D\left(\frac{X_{K-}}{\sqrt{1 - M \cos \varepsilon_K}}\right) \right] \right\}, \tag{28a}$$

$$K \equiv 0,1,2,12. \tag{28b}$$

Calculation of the pressure field is given in Fig. 5(a) for hard ground on the source side and soft ground on the receiver side, and in Fig. 6(a) for soft ground on both sides. Figures 5(b) and 6(b) show the calculation of the SPL for a stationary source in the corresponding geometry, with offset

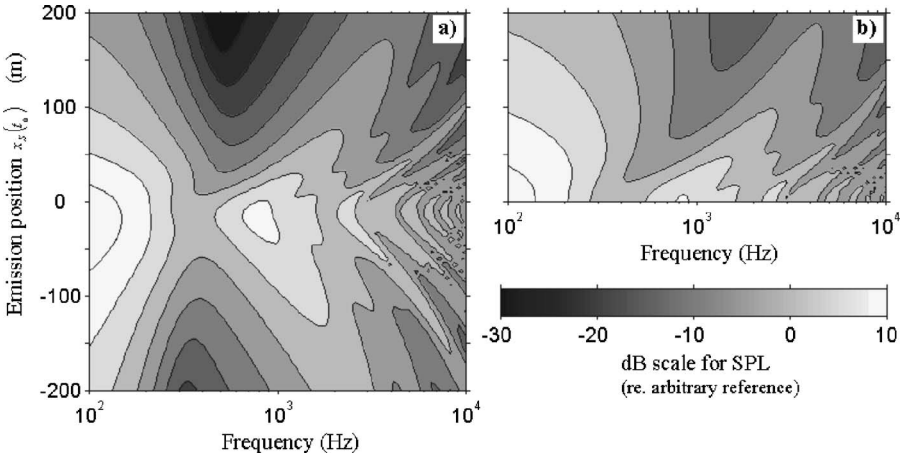

FIG. 6. Same as Fig. 5 but with soft ground on both sides of the barrier.

varying from 0 to 200 m. (The symmetrical pattern for offset −200 m to 0 is not shown). With common y axis, comparing with Figs. 5(a) to 5(b), to 6(a) and 6(b) allows assessing the effect of source convection which are not related to the change of source location along the trajectory—that is the influence of the Doppler and convection factors in the formulation of the sound field. For both Figs. 5 and 6, soft ground is characterized by a two parameter model admittance[17] with flow resistivity $\sigma_e=140$ kPa s m^{-2} and porosity rate $\alpha_e=35$ m^{-1}. The pressure field is found to be asymmetric along the source trajectory. Lower levels are predicted when the source recedes from the receiver $[x_S(t_0)\geqslant 0, (1-M\cos\varepsilon_K)^{-2}\leqslant 1]$, whereas sensitivity of the sound field to source motion is predicted to be more important on source approach $[x_S(t_0)\leqslant 0, (1-M\cos\varepsilon_K)^{-2}\geqslant 1]$, for which the deformation of the SPL pattern is stronger. Expectedly, strong interference between the four components of the acoustic pressure is predicted at high frequencies. The two dips related to the reflections on each side of the barrier are identifiable, particularly at large offsets and for source recession. Comparing Figs. 5 and 6, it is also predicted that sensitivity to motion is somewhat more important for soft ground than it is for hard ground.

C. Source in motion parallel to a ground discontinuity

A semiempirical formula for the sound field due to a stationary source in the presence of a ground discontinuity has been derived by De Jong *et al.*,[6] considering the superposition of two half-planes with different admittance. This model was shown to be valid in 3D situations for which the propagation path is not necessarily perpendicular to the discontinuity,[18] and was later extended to dipole sources.[8] Derivation of the acoustic pressure field for source motion in parallel to the discontinuity is then straightforward, after Eq. (8).

Consider an admittance step coinciding with the x axis, as shown in Fig. 7. Let a source S be in uniform motion at height z_S, in parallel to the discontinuity. The ground on the source side is characterized by its specific admittance β_1 and that on the receiver side by β_2. The direct wave reaching receiver R at time t has been emitted at instant t_e, following path $R=c_0(t-t_e)$ with azimuthal angle ψ and elevation angle ϕ. The reflected wave reaching R at time t (denoted by dashed parameters in the coordinate system attached to the receiver) has been emitted at retarded time t_e' and has followed path $R'=c_0(t-t_e')$ with azimuthal and elevation angles $\psi'=\psi(t_e')$ and $\theta'=\theta(t_e')$, respectively. The expressions for R,ψ,ϕ and R',ψ',θ' are not detailed here for brevity, their derivation from a kinematics analysis for the source and its image with respect to the ground is straightforward.[12,13]

The diffracted wave follows path L as per defined in Eq. (3). Its time of emission t_e'' is calculated after Eqs. (3) and (4). In the following, a double dash denotes corresponding parameters in the coordinate system attached to the receiver.

In the auxiliary coordinate system, the monopole component of the acoustic pressure for a single discontinuity is, after De Jong *et al.*[6]

$$p^{(0)}=\frac{\exp(-i\omega t_L)}{4\pi}\left[\frac{\exp(ik_0R_L)}{R_L}+Q_G'\frac{\exp(ik_0R_L')}{R_L'}+(Q_1'-Q_2')\frac{1+i}{2}\frac{\exp(ik_0L_L)}{L_L}D_L\right], \tag{29a}$$

where L_L is the diffraction path in the auxiliary coordinates for a horizontal half-plane whose edge coincides with the ground discontinuity and $D_L=A_D(X_{L+})+A_D(X_{L-})$ the sum of the two diffraction integrals given in Eq. (10). The quantity Q_G' is the spherical wave reflection coefficient at the point of specular reflection, with $G\equiv 1$ or 2 depending on the geometry. The quantities, Q_1' and Q_2', are the spherical wave reflection coefficients for each type of ground. They are calculated after the Doppler-Weyl-Van der Pol formula[11]

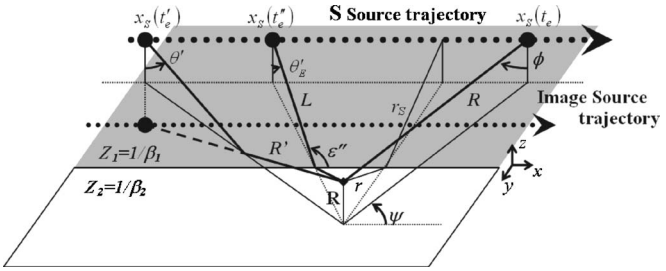

FIG. 7. Geometry for a source in uniform motion in parallel to a ground discontinuity.

$$Q_i' = R_{Pi}' + (1 - R_{Pi}')F\left(\frac{w_i'}{\sqrt{1 - M_R'}}\right), \tag{29b}$$

with M_R' as the component of the Mach number in the direction of propagation of the reflected wave

$$M_R' = M \cos\psi' \sin\theta', \tag{29c}$$

$$R_{Pi}' = \frac{\cos\theta' - \beta_i}{\cos\theta' + \beta_i}. \tag{29d}$$

The expression for the boundary loss function F is analogous to that given in (25c), with

$$w_i' = \left(-\tfrac{1}{2} ik_0 R'\right)^{1/2} (\cos\theta' + \beta_i). \tag{29e}$$

When the point of specular reflection coincides with the admittance step, $R_L' = L_L$ and $X_{L+} = 0$. With $A_D(0) = -(1-i)/2$, the continuity of the monopole component of the acoustic pressure is ensured.

The dipole component is also expressed as the sum of a direct, a reflected, and a diffracted pressure wave to which are applied the appropriate reflection coefficients. The formulation for the direct and the reflected fields are straightforward after Li *et al.*[19] The diffracted wave is calculated after Buret *et al.*[8] and the total dipole contribution is expressed as

$$\begin{aligned} p^{(1)} = \frac{\exp(-i\omega t_L)}{4\pi} \Bigg\{ & \Theta_R \frac{1 - ik_0 R_L}{R_L} \frac{e^{ik_0 R_L}}{R_L} \\ & + \Theta_R' \frac{1 - ik_0 R_L'}{R_L'} \frac{e^{ik_0 R_L'}}{R_L'} Q_G' \\ & + \frac{1+i}{2} \frac{e^{ik_0 L_L}}{L_L} \Bigg[\Theta_L \frac{1 - ik_0 L_L}{L_L} (Q_1' - Q_2') \\ & + \frac{\partial (Q_1' - Q_2')}{\partial x_L} \Bigg] D_L \Bigg\}, \end{aligned} \tag{30a}$$

with the directivity factors given by

$$\begin{aligned} \Theta_R &= \cos\psi_L \sin\phi_L, \\ \Theta_R' &= \cos\psi_L \sin\theta_L', \\ \Theta_E &= \cos\psi_L \sin\theta_{E,L}. \end{aligned} \tag{30b}$$

In the earlier equation, ψ_L, ϕ_L, and θ_L are, respectively, the azimuthal angle, the elevation angles for the direct ray and the elevation angle for the reflected ray in the auxiliary coordinates. The quantity, $\theta_{E,L}$ is the elevation angle of the ray linking the source to the admittance step. Corresponding angles in the coordinates system attached to the receiver are shown in Fig. 7. Remarkably, when the specular reflection occurs at the admittance step: $\Theta_R' = \Theta_E = \cos\varepsilon_L$ and continuity of the acoustic pressure is ensured. The very last term in Eq. (30a) can be neglected, as variations of the spherical wave coefficient in the horizontal directions are known to be small.[8] Equation (30) then simplifies to an expression analogous to that of the monopole component given in Eq. (29).

The total pressure field is derived by substituting Eqs. (29) and (30) into Eq. (8). Transforming back into the coordinate system attached to the receiver is straightforward by means of the relations in Eq. (14) and noting that[11]

$$R_L = \gamma^2 R(1 - M\cos\psi\sin\phi), \quad t_L - \frac{R_L}{c_0} = t - \frac{R}{c_0},$$

$$\Theta_R = \frac{\cos\psi\sin\phi - M}{1 - M\cos\psi\sin\phi}, \tag{31a}$$

$$R_L' = \gamma^2 R'(1 - M\cos\psi'\sin\phi'), \quad t_L - \frac{R_L'}{c_0} = t - \frac{R'}{c_0},$$

$$\Theta_R' = \frac{\cos\psi'\sin\theta' - M}{1 - M\cos\psi'\sin\theta'}, \tag{31b}$$

and

$$\Theta_E = \frac{\cos\varepsilon'' - M}{1 - M\cos\varepsilon''} = \frac{\cos\psi''\sin\theta_E'' - M}{1 - M\cos\psi''\sin\theta''}. \tag{31c}$$

The pressure field for a source in uniform motion along an admittance discontinuity is then expressed as

$$p = p_{\text{dir}} + Q_G p_{\text{refl}} + (Q_1 - Q_2) p_{\text{diffr}}, \tag{32a}$$

where p_{dir}, p_{refl}, and p_{diffr} represent the direct, reflected, and diffracted waves, respectively,

$$\begin{aligned} p_{\text{dir}} = P_0 \frac{\exp(-i\omega t)}{4\pi} & \frac{\exp(ik_0 R)}{R(1 - M\cos\psi\sin\phi)^2} \\ & \times \left[1 - \frac{M}{ik_0 R}\left(\frac{\cos\psi\sin\phi - M}{1 - M\cos\psi\sin\phi}\right)\right], \end{aligned} \tag{32b}$$

$$\begin{aligned} p_{\text{refl}} = P_0 \frac{\exp(-i\omega t)}{4\pi} & \frac{\exp(ik_0 R')}{R'(1 - M\cos\psi'\sin\phi')^2} \\ & \times \left[1 - \frac{M}{ik_0 R'}\left(\frac{\cos\psi'\sin\phi' - M}{1 - M\cos\psi'\sin\phi'}\right)\right], \end{aligned} \tag{32c}$$

$$\begin{aligned} p_{\text{diffr}} = P_0 \frac{\exp(-i\omega t)}{4\pi} & \frac{1+i}{2} \frac{\exp(ik_0 L)}{L(1 - M\cos\psi''\sin\theta_E'')^2} \\ & \times \left[1 - \frac{M}{ik_0 L}\left(\frac{\cos\psi''\sin\theta_E'' - M}{1 - M\cos\psi''\sin\theta_E''}\right)\right] \\ & \times \left[A_D\left(\frac{X_+}{\sqrt{1 - M\cos\psi''\sin\theta_E''}}\right)\right. \\ & \left. + A_D\left(\frac{X_-}{\sqrt{1 - M\cos\psi''\sin\theta_E''}}\right)\right]. \end{aligned} \tag{32d}$$

Figure 8(a) shows the calculation of the SPL calculated according to Eq. (32) as a function of the source position at emission of the reflected wave $x_S(t_e')$ with a 33%-hard ground mix (when the proportion of hard ground below the sound propagation path is 33%). The source is moving at Mach number 0.3 with its track located 10 m away from the admittance step at height 1 m above hard ground. The receiver is located 20 m away from the discontinuity, 1.2 m above soft ground characterized by a two parameter model

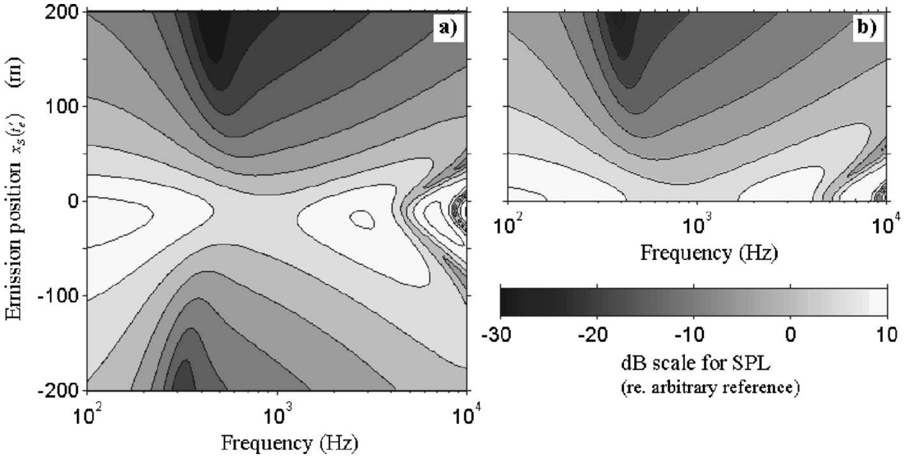

FIG. 8. (a) SPL (re. Arbitrary reference) for a source moving at Mach number 0.3 parallel to an admittance discontinuity, 10 m away from it, at height 1 m. The receiver is 20 m away from the step line at height 1.2 m. The ground on the source side is hard, the ground on the receiver side is characterized by $\sigma_e = 140$ kPa s m^{-2} and $\alpha_e = 35$ m^{-1}. The proportion of the sound path occurring above hard ground is 33%. (b) SPL for a stationary source in the same geometry as in (a), with offset varying from 0 to 200 m.

admittance[17] with flow resistivity $\sigma_e = 140$ kPa s m^{-2} and porosity rate $\alpha_e = 35$ m^{-1}. Figure 8(b) shows the SPL for the corresponding stationary source at offset 0–200 m and allows assessing the effects of source motion. The corresponding instantaneous excess attenuation EA $= 10\log(|p(t)/p_{\mathrm{dir}}(t)|)$ is shown in Fig. 9(a), for the source at offset 100 m on approach $[x_S(t_e') = -100$ m, thick solid line$]$ and recession $[x_S(t_e') = +100$ m; thin solid line$]$ and for the corresponding stationary source (dashed line). In Fig. 9(a), dotted lines of different thickness showing the calculation at closet position $[x_S(t_e') = 0]$ for moving and stationary source, respectively, are coinciding: effects of motion on ground attenuation when the source is close to the receiver can be neglected. Figure 9(b) shows the excess attenuation but for the source track over hard ground 20 m away from the admittance step and receiver over soft ground 10 m away (the proportion of the sound path occurring above hard ground is 66%).

As was noted previously in the case of homogenous ground,[11] the effects of motion are predicted to be small. Again, it is predicted that the SPL shows a dissymmetry along the source motion due to the Doppler shift and the convection factor that affect the location and magnitude of the ground effect dip. As clearly shown in Fig. 9, this is predicted to result in lower SPL than for a stationary source when the source approaches the receiver $[x_S(t_e') \leq 0]$, up to the frequency of the ground effect dip and higher levels from the dip up to the interference in the high frequencies. This trend is reversed when the source recedes from the receiver. On source approach, the ground effect dip is slightly sharper and deeper than that for a stationary source, whereas on recession it is slightly broader and shallower. This is due to the Doppler factor within the argument of the boundary loss factor as given in the Doppler-Weyl-Van der Pol formula [cf. Eq. (29b)]: on source approach the absorbing ground is seen as softer, whereas it is seen as harder on recession. On the other hand, comparing Figs. 9(a) and 9(b), the sound field is predicted to be little affected by the change of the proportion in the ground mix covering the source—receiver path.

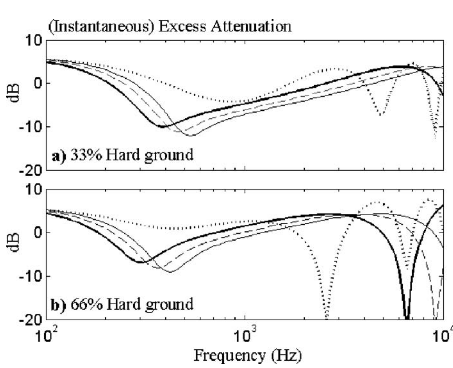

FIG. 9. Instantaneous excess attenuation (a) for the same configurations as in Fig. 8, (b) for a proportion of hard ground over the propagation path of 66% (source path over hard ground 20 m away from the discontinuity, receiver 10 m away, over soft ground). (—) Approaching source $x_S(t_e') = -100$ m, (—) Receding source $x_S(t_e') = 100$ m, (---) stationary source at offset $x_S = 100$ m, (······) moving source at closest separation $[x_S(t_e') = 0]$ and coinciding with the calculation for a stationary source at closest separation (···········).

IV. CONCLUDING REMARKS

It has been shown that the problem of diffraction of the sound field due to a source in motion parallel to a semi-infinite rigid wedge is strongly analogous to the case of a stationary source, as a result of the conservation of the geometry in the cross-sectional plane of the obstacle. By means of an auxiliary coordinate system and the formulations for monopole and dipole sources, a closed-form formula for the diffracted sound field due to a monopole in uniform motion parallel to a diffracting edge has been derived that is similar to Pierce's solution for a stationary monopole and its extension to dipole sources.

Although motion results in dissymmetry of the diffracted pressure along the source trajectory, its effects on barrier attenuation are predicted to be limited. In particular the effects on IL are predicted to be minimal so that design schemes used for stationary sources are valid also for sources in motion.

On the other hand, predictions for the absolute sound pressure levels must account for the influence of the convection and Doppler factors on the resulting sound field.

New models have been derived for propagation of sound due to sources moving parallel to barriers in the presence of the ground and greater sensitivity to motion is predicted on source approach and for softer grounds. De Jong's semi-empirical model for propagation in the presence of a ground discontinuity has been extended also to the case of source

motion along an admittance step. Sensitivity to source motion is also predicted to be stronger on source approach, whereas it is predicted to be little affected by the proportion of hard and soft ground covering the sound propagation path.

Further extensions of this work could include effects of absorptive barriers and impedance strips parallel to the axis of source motion.

ACKNOWLEDGMENTS

This work was prepared when one of the authors (M.B.) was on study leave in the Department of Mechanical Engineering, the Hong Kong Polytechnic University. The authors would like to thank the Research Committees of the Open University and the Hong Kong Polytechnic University for their financial support in this project. M.B. was supported by an Open University Competitive Studentship. One of the authors (K.M.L.) gratefully acknowledges a generous donation from MTR Corporation for partial support of this research.

[1]J. J. Bowman, T. B. A. Senior, and P. L. E. Uslenghi, *Electromagnetic and Acoustic Scattering by Simple Shapes* (North-Holland, Amsterdam, 1969).
[2]U. Kurze, "Noise reduction by barriers," J. Acoust. Soc. Am. **55**(3), 504–518 (1974).
[3]Z. Maekawa, "Noise reduction by screens," Appl. Acoust. **1**, 157–173 (1968).
[4]H. G. Jonasson, "Sound reduction by barriers on the ground," J. Sound Vib. **22**(1), 113–126 (1972).
[5]A. D. Pierce, "Diffraction of sound around corners and wide barriers," J. Acoust. Soc. Am. **55**(5), 941–955 (1974).
[6]B. A. De Jong, A. Moerkerken, and J. D. Van der Toorn, "Propagation of sound over grassland and over an earth barrier," J. Sound Vib. **86**(1), 23–46 (1983).
[7]P. Koers, "Diffraction by an absorbing barrier or by an impedance transition," *Proc. InterNoise 83, 1983*, Vol. **1**, pp. 311–314.
[8]M. Buret, K. M. Li, K. Attenborough, "Diffraction of sound from a dipole source near to a barrier or an impedance discontinuity," J. Acoust. Soc. Am. **113**(5), 2480–2494 (2003).
[9]P. Menounou, J. L. Bush-Vishniac, and D. T. Blackstock, "Directive line source model: A new model for sound diffraction by half planes and wedges," J. Acoust. Soc. Am. **107**(6), 2973–2986 (2000).
[10]R. Makarewicz, J. Jarzecki, K. Berezowska-Apolinarska, and A. Preis, "Rail transportation noise with and without a barrier," Appl. Acoust. **26**, 135–147 (1989).
[11]M. Buret, K. M. Li, and K. Attenborough, "Optimisation of ground attenuation for moving sources," Appl. Acoust. **67**(2), 135–157 (2006).
[12]K. M. Li, M. Buret, and K. Attenborough, "The propagation of sound due to a source moving at high speed in a refracting medium," *Proc. Euronoise 98, 1998*, Vol. **2**, pp. 955–960.
[13]P. M. Morse and K. U. Ingard, *Theoretical Acoustics* (McGraw Hill, New York, 1968).
[14]A typographical error in Eq. (11.2.15) of Ref. 13 should be corrected. The denominator for the second term should read $R^2(1-\mathrm{M}\cos\theta)^3$ [in place of $R^2(1-\mathrm{M}\cos\theta)^2$].
[15]A. D. Pierce, *Acoustics, An Introduction to Its Physical Principles and Applications* (Acoustical Society of America, New York, 1989).
[16]The orientation of dipole missing in Eq. 14a of Ref. 8 has been added in Eq. 11 where its direction cosines (ℓ_x,ℓ_y,ℓ_z) are given by $(\cos\varepsilon_L,0,0)$ in the present situation.
[17]R. Raspet and J. M. Sabatier, "The surface impedance of grounds with exponential porosity profiles," J. Acoust. Soc. Am. **99**(1), 147–152 (1996).
[18]D. C. Hothershall and J. N. B. Harriot, "Approximate models for sound propagation above multi-impedance plane boundaries," J. Acoust. Soc. Am. **97**(2), 918–926 (1995).
[19]K. M. Li, S. Taherzadeh, and K. Attenborough, "Sound propagation from a dipole source near an impedance plane," J. Acoust. Soc. Am. **101**(6), 3343–3352 (1997).